Acetylide Complexes of Diamagnetic Gallium(III) and Paramagnetic Iron(III) Porphyrins†

Alan L. Balch,*,‡ Lechosław Latos-Grażyński,§ Bruce C. Noll,‡ and Shane L. Phillips‡

Department of Chemistry, University of California, Davis, California 95616, and Institute of Chemistry, University of Wrocław, Wrocław, 58383 Poland

Received August 25, 1992

Five-coordinate {(TPP)Ga^{III}(C≡CR)} complexes (TPP is the dianion of tetraphenylporphyrin; R is *n*-Pr or Ph) and {(TTP)Fe^{III}(C≡CR)} (TPP is the dianion of tetrakis(*p*-tolyl)porphyrin); R = *n*-Pr or Ph) have been obtained by the reaction of {(P)M^{III}Cl} (M = Ga or Fe, P = porphyrin dianion) with the appropriate lithium acetylide. Red blocks of {(TPP)Ga^{III}(C≡CPr^n)} ($C_{49}H_{35}GaN_4$) crystallize in the orthorhombic space group $Pna2_1$ with a = 12.032(2) Å, b = 27.502(5) Å, and c = 11.138(2) Å at 120 K with Z = 4. Refinement of 487 parameters with 2818 reflections gave R = 0.043 and R_w = 0.040. The complex consists of the five-coordinate gallium bound to a saddle-shaped porphyrin (Ga–N distance (average) = 2.047 Å) and a linear axial propyl acetylide (Ga–C distance = 1.949(6) Å). The iron complexes decompose during attempts at chromatographic purifications and consequently have been examined only in solution. In noncoordinating solvents (toluene, dichloromethane) they exhibit ^{1}H NMR spectra that are characteristic of high-spin ($S = {}^5/_2$) species rather than the low-spin ($S = {}^1/_2$) ground state found for similar complexes with axial alkyl or aryl substituents. Addition of tetrahydrofuran (THF) or pyridine (py) results in the conversion to low-spin ($S = {}^1/_2$), six-coordinate species, {B(TTP)Fe^{III}(C≡CR)} (B = THF or py). The iron(III) acetylide complexes are not reactive toward dioxygen but are converted into {(TTP)Fe^{III}Br} when treated with bromine in toluene solution.

Introduction

Despite considerable interest in organometallic derivatives of metalloporphyrins,[1-3] there has been little attention given to the formation of iron complexes with acetylene or acetylide ions as axial substituents. Cytochrome P-450 is believed to be responsible for the oxidative conversion of terminal acetylenes to carboxylic acids.[4] Terminal acetylenes are also known to be involved in the destruction of the heme in cytochrome P450 through the formation of N-substituted porphyrins.[4,5] The currently accepted mechanism for these transformations involves attack of the electrophilic, highly oxidized iron porphyrin prosthetic group on the π bond of the olefin.[5] It has also been suggested that carbene complexes derived from oxidation of an acetylene might be involved in this process.[4]

The oxidation of iron porphyrin complexes with axial aryl ligands {PFe^{III}Ar} is a complex process that can result in transfer of the aryl substituent from iron to nitrogen and thereby yield an N-substituted porphyrin.[6-9] In the present work we undertook an examination of iron porphyrins with axial acetylide groups in order to see if a similar iron-to-nitrogen transfer of the acetylide might occur upon oxidation. This necessitated the preparation and characterization of acetylide complexes of the type {PFe^{III}-(C≡CR)}. Initially it was expected that these would resemble their alkyl and aryl counterparts. The alkyl complexes {PFe^{III}R} are low-spin ($S = {}^1/_2$), complexes with a 15-electron count at iron.[10,11] The methyl derivative {(TPP)Fe^{III}Me} has been subject to thorough structural characterization by X-ray crystallography.[12] This showed the metal was five-coordinate with the iron 0.15 Å out of the N_4 plane as is characteristic of low-spin species.[12] The ^{1}H NMR spectra of these paramagnetic complexes have been thoroughly analyzed.[13,14] They exhibit an upfield pyrrole resonance (at ca. −34 ppm at −70 °C) with large downfield hyperfine shifts for the α protons and upfield shifts for the β protons of the axial alkyl groups. These alkyl complexes are extremely sensitive to dioxygen.[13,15,16] At low temperature, it has been possible to detect their conversion into high-spin complexes with axial alkyl hydroperoxide groups coordinated to iron. Most of the iron(III) complexes with axial aryl groups are also low-spin. {(TPP)Fe^{III}Ph} has been subject to structural characterization by X-ray crystallography and shows the typical features of a low-spin complex.[17] Likewise the ^{1}H NMR spectra

Table I. Electronic Absorption Spectra

compd	λ_{max}, nm (ϵ, cm^{-1} M^{-1})
{(TPP)Ga^{III}(C≡CPr^n)}	428 (58 × 10^4), 408 sh (37 × 10^3), 560 (19 × 10^3), 600 (61 × 10^2)
{(TPP)Ga^{III}(C≡CPh)}	428 (41 × 10^4), 408 sh (32 × 10^3), 560 (15 × 10^3), 600 (54 × 10^2)
{(TPP)Ga^{III}($(CH_2)_4$-CH=CH_2)}[a]	442 (27 × 10^4), 536 (35 × 10^3), 576 (11 × 10^3), 618 (9.4 × 10^2)
{(TPP)Ga^{III}(OAc)}[b]	414 (13 × 10^4), 549 (74 × 10^2), 568 (33 × 10^2)
{(TTP)Fe^{III}(C≡CPr^n)}	424 (25),[c] 506 (3.3),[c] 566 (1.3),[c] 696 (1)[c]
{(TTP)Fe^{III}(C≡CPh)}	420 (33),[c] 510 (4.2),[c] 568 (2.6),[c] 716(1)[c]

[a] Data from ref 26. [b] Data from ref 23. [c] Relative values.

† Abbreviations used: P, generic porphyrin dianion; R, alkyl group; Ar, aryl group; TPP, dianion of *meso*-tetraphenylporphyrin; TTP, dianion of *meso*-tetrakis(*p*-tolyl)porphyrin; OEP, dianion of octaethylporphyrin; THF, tetrahydrofuran; py, pyridine, Im, imidazole.

‡ University of California.

§ University of Wrocław.

(1) Guilard, R.; Kadish, K. M. *Chem. Revs.* **1988**, *88*, 1121.
(2) Guilard, R.; Lecomte, C.; Kadish, K. M. *Struct. Bonding* **1987**, *64*, 205.
(3) Brothers, P. J.; Collman, J. P. *Acc. Chem. Res.* **1986**, *19*, 209.
(4) Ortiz de Montellano, P. R. In *Bioactivation of Foreign Compounds* Anders, M. W., Ed.; Academic Press: New York, 1985; p 121.
(5) Ortiz de Montellano, P. R.; Kunze, K. L.; Beilan, H. S.; Wheeler, C. *Biochemistry* **1982**, *21*, 1331.
(6) Kunze, K. L.; Ortiz de Montellano, P. R. *J. Am. Chem. Soc.* **1983**, *105*, 1380.
(7) Lançon, D.; Cocolios, P.; Guilard, R.; Kadish, K. M. *J. Am. Chem. Soc.* **1984**, *106*, 4472.
(8) Balch, A. L.; Renner, M. W. *J. Am. Chem. Soc.* **1986**, *108*, 2603.
(9) Arasasingham, R. D.; Balch, A. L.; Hart, R. L.; Latos-Grażyński, L. *J. Am. Chem. Soc.* **1990**, *112*, 7566.
(10) Lexa, D.; Mispelter, J.; Savéant, J.-M. *J. Am. Chem. Soc.* **1981**, *103*, 6806.
(11) Cocolios, P.; Lagrange, G.; Guilard, R. *J. Organomet. Chem.* **1983**, *253*, 65.
(12) Balch, A. L.; Olmstead, M. M.; Safari, N. To be published.
(13) Balch, A. L.; Hart, R. L.; Latos-Grażyński, L., Traylor, T. G. *J. Am. Chem. Soc.* **1990**, *112*, 7382.
(14) Li, Z.; Goff, H. M. *Inorg. Chem.* **1992**, *31*, 1547.
(15) Arasasingham, R. D.; Balch, A. L.; Cornman, C. R.; Latos-Grażyński, L. *J. Am. Chem. Soc.* **1989**, *111*, 4357. Arasasingham, R. D.; Balch, A. L.; Latos-Grażyński, L. *J. Am. Chem. Soc.* **1987**, *109*, 5846.
(16) Balch, A. L. *Inorg. Chim. Acta* **1992**, *198–200*, 297.

0020-1669/93/1332-1124$04.00/0 © 1993 American Chemical Society

Table II. ^{1}H-NMR Spectral Data

		chem shift (ppm)						
			axial ligand[f]			TPP-Ph[f]		
compd	*T*	pyrr	*o* or α	*m* or β	*p* or γ	*o*	*m*	*p*
{(TPP)Ga^{III}(C≡CPh)}[a]	23	9.10 (s)	5.65 (d)	6.04 (t)	6.18 (t)	8.04 (d)	7.37–7.50 (m)	
{(TPP)Ga^{III}(C≡CPr^n)}[a]	23	9.09 (s)	0.08 (t)	−0.17 (h)	−0.40 (t)	8.05 (t)	7.38–7.50 (m)	
{(TPP)Fe^{III}(C≡CPh)}[b]	−70	93.3	−83.9	48.9	−77.8	*d*	13.8, 12.5	6.9[e]
{(THF)(TTP)Fe^{III}(C≡CPh)}[b]	−70	−26.9	−15.6	31.8	−19.4			
{(py)(TTP)Fe^{III}(C≡CPh)}[c]	−70	−31.9	−9.5	32.9	−13.8	−0.6, −1.7	3.2, 2.0	−1.3[e]
{(TTP)Fe^{III}(C≡CPr^n)}[c]	20	73.1	*d*	*d*	*d*	*d*	10.4, 11.3	5.2
{(py)(TTP)Fe^{III}(C≡CPr^n)}[c]	−70	−32.4	318 (br)	21.2 (s)	14.5 (s)	−1.9, −0.2	2.8, 2.5	−0.6
{(TTP)Fe^{III}(OPh)}[c]	−30	98	−147	116	−136			
	−70	118.5		136.7	−164.1			
{(TTP)Fe^{III}Ph}[c]	−30	−24	−95	18	−31			
	−70	−32.5	−108.5	23.1	−34.4			

[a] d_6-benzene. [b] d_2-dichloromethane. [c] d_8-toluene. [d] Not observed presumably due to large line width. [e] Methyl resonance. [f] d, doublet; t, triplet; h, hextet; s, singlet; br, broad; m, multiplet.

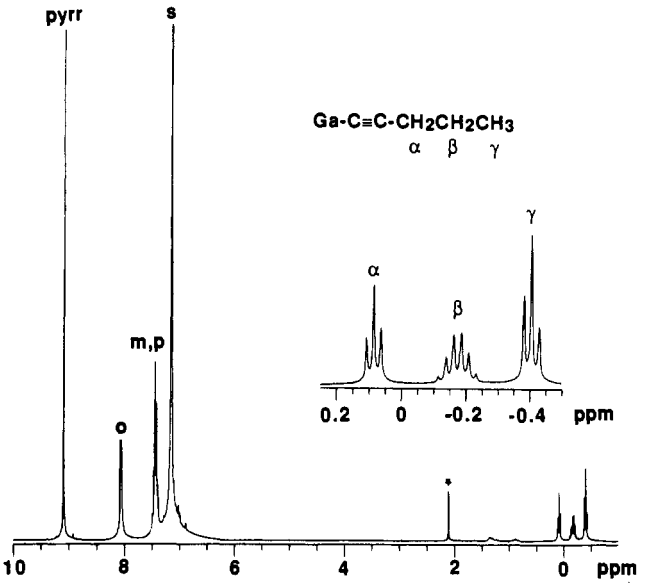

Figure 1. 300-MHz ^{1}H NMR spectrum of {(TPP)Ga^{III}(C≡CPr^n)} in benzene-d_6 at 23 °C. Resonances are identified as pyrr, pyrrole protons; o, m, p, *ortho*, *meta*, *para* phenyl protons; α, β, γ, propyl protons; S, solvent; ✱, solvent impurity. The inset shows an expansion of the region of the propyl resonances.

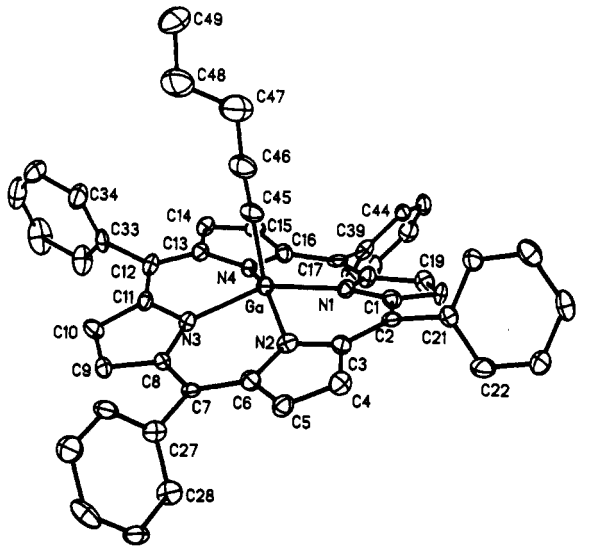

Figure 2. Perspective view of {(TPP)Ga^{III}(C≡CPr^n)} showing 50% thermal contours for all atoms.

of most aryl derivatives show relatively narrow upfield pyrrole resonances,[11,18,19] that are characteristic of low-spin heme derivatives like [TPPFe^{III}(CN)$_2$]$^-$ [20] or [(TPP)Fe^{III}(Im)$_2$]$^+$,[21] and aryl resonances that are indicative of π unpaired spin density in that group. These include downfield hyperfine shifts for the *meta* aryl protons and upfield shifts for the *ortho* and *para* aryl protons. Complexes with a axial perfluorophenyl group, however, are exceptional.[22] These have characteristics of high-spin ($S = {}^5/_2$) complexes. In particular their ^{1}H NMR show broad pyrrole resonances that have downfield hyperfine shifts.

In this work we have used the general route of reaction of {PM^{III}Cl} with a lithium acetylide as the route to the formation of the desired acetylide complexes. Since the iron(III) derivatives proved difficult to purify, their gallium(III) counterparts were also synthesized to provide more stable models. Gallium(III) porphyrin complexes with an axial phenyl acetylide have been previously described.[23]

Results

Preparation and Characterization of Gallium(III) Complexes. The gallium complexes, {(TPP)Ga^{III}(C≡CR)} (R = *n*-Pr or Ph), were prepared by the addition of the appropriate lithium acetylide to a toluene solution of {(TPP)Ga^{III}Cl}. The complexes were isolated as deep red, crystalline powders which have good solubility in benzene, dichloromethane and chloroform, but have low solubility in *n*-hexane or diethyl ether. These acetylide complexes, like their alkyl counterparts,[24–26] are stable to air even in dilute solution.

The electronic absorption spectra of the complexes, which are presented in Table I, are characteristic of porphyrin complexes with an intense Soret peak at 428 nm. Dilute solutions of the complex are yellow while more concentrated solutions are violet. The absorption spectra, however, are not concentration dependent. The absorption spectra are similar to those of other gallium porphyrins with either halide or alkoxide axial ligands.[23] However, they are quite different from the spectra of the green alkyl complexes {(TPP)Ga^{III}R} which have their Soret band at longer wavelength (ca. 442 nm).

^{1}H NMR spectroscopic data for these acetylide complexes are reported in Table II. The spectrum for {(TPP)Ga^{III}(C≡CPr^n)}

(17) Doppelt, P. *Inorg. Chem.* **1984**, *23*, 4009.
(18) Balch, A. L.; Renner, M. W. *Inorg. Chem.* **1986**, *25*, 303.
(19) Lançon, D.; Cocolios, P.; Guilard, R.; Kadish, K. M. *Organometallics* **1984**, *3*, 1164.
(20) Del Gaudio, J.; LaMar, G. N. *J. Am. Chem. Soc.* **1976**, *98*, 3014.
(21) Satterlee, J. D.; LaMar, G. N. *J. Am. Chem. Soc.* **1976**, *98*, 2804. LaMar, G. N.; Walker, F. A. *J. Am. Chem. Soc.* **1973**, *95*, 1782.
(22) Guilard, R.; Boisselier-Cocolios, B.; Tabard, A.; Cocolois, P.; Simonet, B.; Kadish, K. M. *Inorg. Chem.* **1985**, *24*, 2509.
(23) Kadish, K. M.; Cornillon, J.-L.; Coutsolelos, A.; Guilard, R. *Inorg. Chem.* **1987**, *26*, 4167.
(24) Coutsolelos, A.; Guilard, R. *J. Organomet. Chem.* **1983**, *253*, 273.
(25) Kadish, K. M.; Boisselier-Cocolios, B.; Coutsolelos, A.; Mitaine, P.; Guilard, R. *Inorg. Chem.* **1985**, *24*, 4521.
(26) Balch, A. L.; Hart, R. L.; Parkin, S. *Inorg. Chim. Acta* **1993**, *205*, 137.

Table III. Atomic Coordinates ($\times 10^4$) and Equivalent Isotropic Displacement Coefficients ($Å^2 \times 10^3$) for {(TPP)Ga^{III}(C≡CPr^n)}

	x	y	z	U(eq)[a]
Ga	6766(1)	3686(1)	4990(1)	17(1)
N(1)	5238(4)	3894(2)	4362(5)	17(2)
N(2)	6156(3)	2992(2)	4983(7)	19(1)
N(3)	7760(4)	3477(2)	6375(5)	16(2)
N(4)	6867(4)	4374(2)	5710(4)	16(1)
C(1)	4557(5)	3603(2)	3677(6)	19(2)
C(2)	4698(5)	3104(2)	3466(5)	20(2)
C(3)	5406(5)	2818(2)	4165(6)	19(2)
C(4)	5360(5)	2298(2)	4219(6)	23(2)
C(5)	6080(4)	2156(2)	5081(8)	23(2)
C(6)	6580(5)	2583(2)	5569(6)	20(2)
C(7)	7406(5)	2591(2)	6462(5)	14(2)
C(8)	7952(5)	3012(2)	6831(6)	18(2)
C(9)	8842(5)	3032(2)	7687(6)	22(2)
C(10)	9240(6)	3494(2)	7684(6)	24(2)
C(11)	8566(5)	3769(2)	6859(6)	18(2)
C(12)	8676(5)	4265(2)	6698(6)	21(2)
C(13)	7829(5)	4554(2)	6191(6)	18(2)
C(14)	7801(5)	5073(2)	6234(6)	21(2)
C(15)	6797(5)	5206(2)	5821(6)	23(2)
C(16)	6209(5)	4773(2)	5464(6)	20(2)
C(17)	5164(4)	4760(2)	4945(8)	20(2)
C(18)	4717(5)	4338(2)	4412(6)	22(2)
C(19)	3674(5)	4316(2)	3788(6)	25(2)
C(20)	3605(5)	3871(2)	3317(6)	21(2)
C(21)	4004(5)	2887(2)	2494(6)	18(2)
C(22)	3128(6)	2566(3)	2720(6)	30(2)
C(23)	2485(6)	2397(2)	1797(6)	29(2)
C(24)	2697(6)	2531(3)	622(6)	29(2)
C(25)	3569(5)	2846(2)	384(6)	30(2)
C(26)	4199(6)	3026(2)	1321(6)	25(2)
C(27)	7786(6)	2118(2)	6964(6)	22(2)
C(28)	7060(5)	1821(2)	7583(6)	26(2)
C(29)	7393(6)	1369(2)	8011(6)	29(2)
C(30)	8463(6)	1216(3)	7817(7)	36(3)
C(31)	9206(6)	1511(3)	7193(6)	34(2)
C(32)	8856(6)	1953(2)	6763(6)	26(2)
C(33)	9710(5)	4512(2)	7105(6)	21(2)
C(34)	10632(6)	4499(3)	6389(8)	35(2)
C(35)	11606(6)	4744(3)	6703(8)	43(3)
C(36)	11647(7)	4991(3)	7755(9)	47(3)
C(37)	10745(7)	5007(3)	8506(8)	50(3)
C(38)	9767(6)	4767(3)	8180(7)	37(3)
C(39)	4507(4)	5224(2)	4917(8)	20(2)
C(40)	4256(7)	5456(3)	5982(7)	24(2)
C(41)	3664(7)	5886(3)	5989(8)	29(3)
C(42)	3331(5)	6094(2)	4922(10)	32(2)
C(43)	3585(7)	5872(3)	3852(8)	27(3)
C(44)	4169(6)	5438(3)	3831(7)	19(2)
C(45)	7812(5)	3702(2)	3654(6)	23(2)
C(46)	8467(6)	3715(3)	2847(7)	34(2)
C(47)	9195(7)	3695(3)	1771(8)	58(3)
C(48)	10359(7)	3771(3)	2011(8)	54(3)
C(49)	11032(6)	3714(3)	821(7)	53(3)

[a] Equivalent isotropic U defined as one-third of the trace of the orthogonalized U_{ij} tensor.

is shown in Figure 1. Each complex shows a single sharp pyrrole resonance at ca 9.2 ppm, a doublet at 8 ppm for the *ortho* phenyl protons and a multiplet at 7.4 ppm for the *meta*- and *para*-phenyl protons of the porphyrin. The axial ligand protons show up-field shifts due to the ring current of the porphyrin. For the *n*-propyl derivative, these appear in the 0.2 to −0.5 ppm range. The resonance assignments in Figure 1 are readily made on the basis of spin-spin splitting and integrated intensity. Thus the methyl resonances are those at highest field while the α-methylene resonances appear as a triplet at ca. 0.1 ppm.

Structure of {(TPP)Ga^{III}(C≡CPr^n)}. The structure of the complex has been determined by X-ray crystallography. A view of the complex is shown in Figure 2. Atomic positional parameters are given in Table III. Table IV contains selected interatomic distances and angles. The complex possesses no crystallographically imposed symmetry.

Table IV. Selected Interatomic Distances and Angles in {(TPP)Ga(C≡CPr^n)}

Distances (Å)			
Ga–N(1)	2.049(5)	Ga–N(2)	2.046(4)
Ga–N(3)	2.035(5)	Ga–N(4)	2.059(5)
Ga–C(45)	1.949(6)		
C(45)–C(46)	1.196(10)	C(46)–C(47)	1.485(11)
C(47)–C(48)	1.441(12)	C(48)–C(49)	1.561(12)
Angles (deg)			
N(1)–Ga–N(2)	86.4(2)	N(1)–Ga–N(3)	149.9(2)
N(2)–Ga–N(3)	87.1(2)	N(1)–Ga–N(4)	85.9(2)
N(2)–Ga–N(4)	151.7(2)	N(3)–Ga–N(4)	86.0(2)
N(1)–Ga–C(45)	108.1(2)	N(2)–Ga–C(45)	104.8(3)
N(3)–Ga–C(45)	102.0(2)	N(4)–Ga–C(45)	103.4(2)
Ga–C(45)–C(46)	178.8(6)	C(45)–C(46)–C(47)	174.0(8)
C(46)–C(47)–C(48)	114.7(7)	C(47)–C(48)–C(49)	109.4(7)

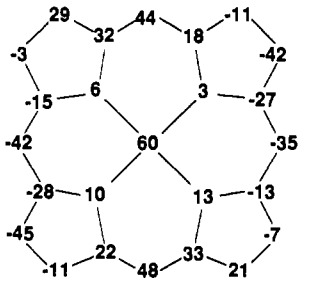

Figure 3. Formal diagram for the porphyrin core of {(TTP)Ga^{III}(C≡CPr^n)} in which each atom symbol is replaced by a number showing the displacement (in 0.01 Å) of that atom from the mean plane of the porphyrin.

The gallium is five-coordinate with the acetylide acting, as expected, as an axial ligand. The Ga–C(45)–C(46) and C(45)–C(46)–C(47) angles (178.8(6), 174.0(8)° respectively) are nearly linear. The Ga–C(45) distance (1.949(6) Å) is slightly shorter than the Ga–C distance (1.992(6) Å) in the cyclopentylmethyl complex, {(TPP)Ga^{III}($CH_2CH(CH_2)_4$)}·$C_6H_5CH_3$.[26] This shortening may result from a combination of electronic and steric effects. The sp hybridization of the acetylide carbon should result in a shortening of the Ga–C bond in comparison to the case of an sp^3 hybridized carbon of an alkyl ligand. The acetylide group, with its linear C(45)C(46)C(47) portion, positions the axial substituent away from the porphyrin plane more effectively than the bent geometry of the cyclopentylmethyl group. The average Ga–N distance (2.047 Å) is also shorter than the average Ga–N distance (2.100 Å) in {(TPP)Ga^{III}($CH_2CH(CH_2)_4$)},[26] but it is similar to those of other gallium(III) porphyrin complexes: {(OEP)Ga^{III}(N_3)}, 2.035 Å;[27] {(OEP)Ga^{III}(SO_3CH_3)} 2.013 A;[28] {(TPP)Ga^{III}Cl}, 2.021 Å.[29]

The porphyrin is saddle shaped. This can be seen qualitatively in Figure 2 and quantitatively in Figure 3, which shows the displacements (in 0.01 Å) of each atom of the porphyrin from the porphyrin mean plane.

Preparation and Characterization of Iron(III) Complexes. The iron acetylide complexes {(TTP)Fe^{III}(C≡CR)} (R = Ph or *n*-Pr) were also obtained by treating a toluene or benzene solution of {(TTP)Fe^{III}Cl} with a solution of the lithium acetylide in tetrahydrofuran. As expected these were more reactive than their gallium counterparts and purification was difficult. Attempts at chromatography, which is effective in purifying iron alkyl complexes, {(TTP)Fe^{III}R},[13,15] were thwarted by ready decomposition on the column. Traces of {(TTP)Fe^{II}} and {(TTP)Fe^{III}}$_2$O that were present were also not removed by crystallization.

(27) Coutsolelos, A.; Guilard, R.; Boukhris, A.; Lecomte, C. *J. Chem. Soc., Dalton Trans.* **1986**, 1779.
(28) Boukhris, A.; Lecomte, A.; Coutsolelos, A.; Guilard, R. *J. Organomet. Chem.* **1986**, *303*, 151.
(29) Coutsolelos, A.; Guilard, R.; Bayeul, D.; Lecomte, C. *Polyhedron.* **1986**, *5*, 1157.

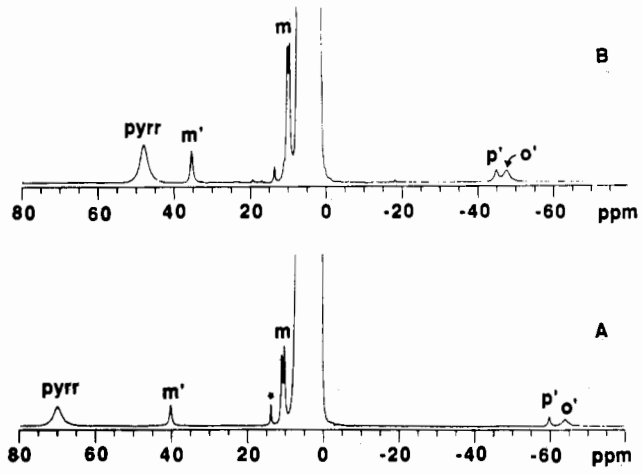

Figure 4. 300-MHz ^{1}H NMR spectrum of (A) {(TTP)Fe^{III}(C≡CPh)} (10 mM) in toluene-d_8 at 23 °C and (B) the same with 30 equivalents of tetrahydrofuran added. Resonances are identified as pyrr, pyrrole protons, o', m', and p', *ortho*, *meta* and *para* phenyl resonances of the axial acetylide; m, *meta* TTP phenyl resonances; ✱, pyrrole of {(TTP)-Fe^{III}OFe^{III}(TTP)}.

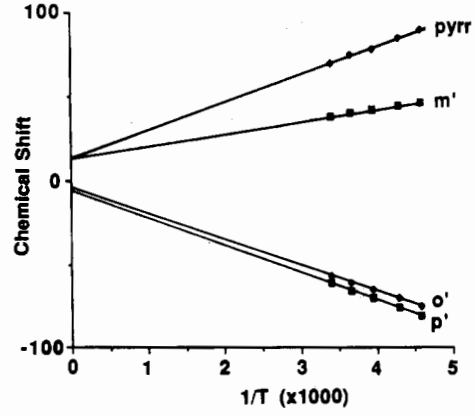

Figure 5. Plot of chemical shift versus $1/T$(K) for {(TTP)Fe^{III}(C≡CPh)} in toluene-d_8 solution. Labels follow those in Figure 4.

Consequently, samples of these complexes were prepared by careful titration with the lithium reagent utilizing ^{1}H NMR spectroscopy to monitor the course of reaction. It was important to avoid addition of any excess of the lithium acetylide, since this causes reduction and formation of {(TTP)Fe^{II}}. After a successful titration, the product solution was carefully decanted from solids that may have precipitated and the sample evaporated to dryness. In this fashion it was possible to remove THF from the complex. The compound was then redissolved in a suitable solvent for further spectroscopic observation.

Electronic absorption spectral data for these iron complexes are given in Table I. Relevant ^{1}H NMR data are presented in Table II. Trace A of Figure 4 shows a ^{1}H NMR spectrum of a toluene solution of a sample of {(TTP)Fe^{III}(C≡CPh)} from which all THF was previously removed. The spectrum has features that are characteristic of the presence of a high-spin ($S = {}^5/_2$), five-coordinate iron(III) porphyrin complex. Thus the resonance at 70 ppm is the pyrrole resonance and the doublet at 12 ppm is the resonance of the *meta*-phenyl protons of the TTP ligand. Similar features are seen in the ^{1}H NMR spectra of other high-spin, five-coordinate complexes (e.g. {(TTP)Fe^{III}Cl}.[30-32] The strongly shifted resonances at 40, –60 and –64 ppm are due to the axial acetylide. These resonances are absent in the spectrum of {(TTP)Fe(C≡CPr^n)} (vide infra). On the basis of its intensity, the peak at –60 ppm is assigned to the *para*-proton of the axial

(30) Walker, F. A.; LaMar, G. N. *Ann. N. Y. Acad. Sci.* **1973**, *266*, 328.
(31) LaMar, G. N.; Walker, F. A. *J. Am. Chem. Soc.* **1973**, *95*, 6950.
(32) LaMar, G. N.; Walker, F. A. *J. Am. Chem. Soc.* **1975**, *97*, 5103.

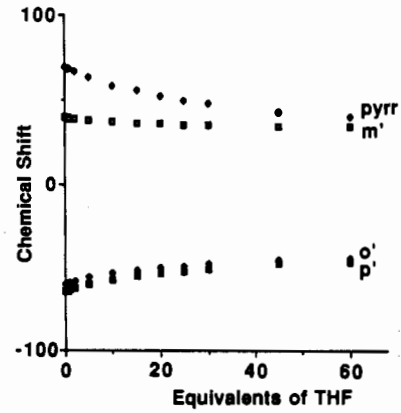

Figure 6. Effect of addition of THF to the ^{1}H NMR resonances of a 10 mM solution of {(TTP)Fe^{III}(C≡CPh)} in toluene-d_8 at 23 °C.

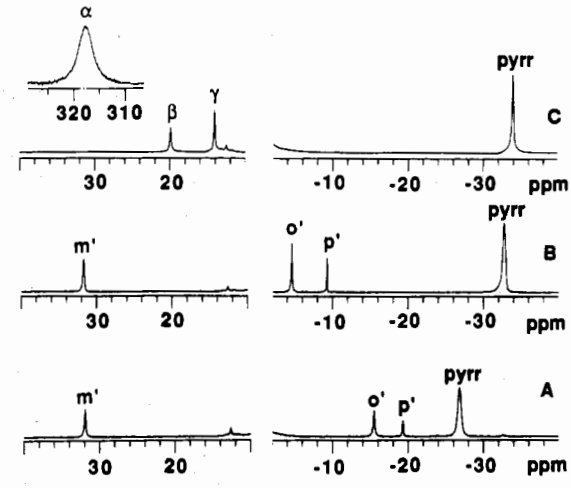

Figure 7. 300-MHz ^{1}H NMR spectra of (A) {THF(TTP)Fe^{III}(C≡CPh)} in dichloromethane-d_2/THF at –70 °C; (B) {py(TTP)Fe^{III}(C≡CPh)} in dichloromethane-d_2/pyridine-d_5 at –70°, and (C) {py(TTP)Fe^{III}(C≡CPr^n)} in dichloromethane-d_2/pyridine-d_5 at –70 °C. Resonance labels follow those in Figures 1 and 4.

phenyl acetylide. On the basis of its greater line width, the resonance at –64 ppm is assigned to the ortho protons of the phenyl acetylide.[33] Then the remaining resonance at 40 ppm is assigned to the meta protons of the axial ligand. The effect of temperature on the spectrum of {(TTP)Fe^{III}(C≡CPh)} is shown in the Curie plot in Figure 5. Over the temperature range that was examined, the chemical shifts are nearly a linear function of $1/T$. The slight curvature seen for other high-spin complexes is not apparent.

Addition of tetrahydrofuran to samples of {(TTP)Fe^{III}-(C≡CPh)} causes pronounced changes. Understanding of these is particularly important since the iron acetylide complexes are initially prepared in the presence of THF (the solvent for the lithium acetylide) and our initial examination of the titration of {(TTP)Fe^{III}Cl} with lithium phenyl acetylide was complicated by a combination of two factors, the Fe/acetylide ratio and the solvent composition. The effect of the THF can be seen by comparing trace A of Figure 4 with trace B which shows a sample to which THF has been added. The presence of THF results in a shift of the pyrrole and axial ligand resonances toward the diamagnetic region. Figure 6 shows a plot of the chemical shift for the pyrrole and axial ligand resonances versus the amount of THF added to the sample of {(TTP)Fe^{III}(C≡CPh)} in toluene at 23 °C.

The effect of lowering the temperature of a sample of {(TTP)-Fe^{III}(C≡CPh)} in the presence of THF is shown in Figure 7.

(33) If we assume that dipolar relaxation is dominant, then relative line widths are proportional to r^6, where r is the iron–proton distance: Swift, T. J. In *NMR of Paramagnetic Molecules*; LaMar, G. N.; Horrocks, W. D., Jr., Holm, R. H. Eds.; Academic Press: New York, 1973; p 59.

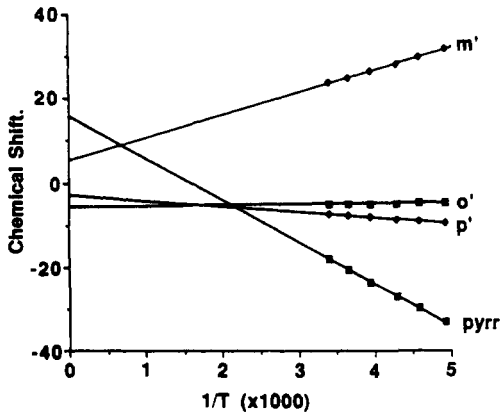

Figure 8. Plot of chemical shift versus $1/T$ (K) for {py(TTP)Fe^{III}(C≡CPh)} in toluene-d_8/pyridine-d_5 solution.

Trace A shows the ^{1}H NMR spectrum of such a sample at −70 °C. The position of the pyrrole resonance is particularly significant. For high-spin {(TTP)Fe^{III}(C≡CPh)}, this resonance is found downfield (at 90 ppm at −70 °C) but in the presence of THF it is found upfield (at −26.5 ppm). The spectrum is indicative of the presence of a low-spin ($S = {}^1/_2$) species. The axial ligand gives rise to resonances at 32, −15.7 and −19.5 ppm. The resonance at −19.5 ppm is assigned to the *para*-phenyl proton on the basis of its intensity. Comparison with other spectra in this figure and Figure 4 suggests that the downfield resonance is due to the *meta*-phenyl protons and the upfield resonance is due to the *ortho*-phenyl protons.

Related spectral changes are observed when pyridine is added to samples of {(TTP)Fe^{III}(C≡CR)}. Trace B of Figure 7 shows the ^{1}H NMR spectrum (recorded at −70 °C) of {py(TTP)Fe^{III}(C≡CPh)} which was formed by adding pyridine-d_5 to a sample of {(TTP)Fe^{III}(C≡CPh)} in dichloromethane-d_2. The spectrum is similar to that of the THF adduct shown in trace A and is characteristic of low-spin ($S = {}^1/_2$), six-coordinate complexes such as [PFe^{III}(Im)$_2$]$^+$,[21] {PFe^{III}(CN)$_2$}$^-$,[20] {(Im)PFe^{III}Ph},[18] and {(Im)PFe^{III}Et}.[15] Thus the pyrrole resonance is located upfield at −32.2 ppm and the resonances of the TTP tolyl groups exhibit small hyperfine shifts that confine them to the crowded 10–0 ppm region, which is not shown in this figure. The resonances of the axial phenyl group show one resonance that is shifted down-field and two that are shifted upfield. That at −9.1 ppm is the *para*-phenyl proton on the basis of its intensity. Trace C of Figure 7 shows the spectrum of {py(TTP)Fe^{III}(C≡CPr^n)} that was obtained by adding pyridine-d_5 to a dichloromethane solution of the complex. Comparison of this spectrum with that in trace B confirms the assignment of the axial phenyl resonances. Those resonances are absent in trace C, where three new resonances are observed in the downfield region. One of these (at 317 ppm) displays a very large hyperfine shift and can confidently be assigned to the α-propyl protons on the basis of this shift and its line width (900 Hz). The resonance at 20 ppm, which is broader than the resonance at 26 ppm, is assigned to the β-propyl protons.[33]

The effect of temperature on the ^{1}H NMR spectrum of {py(TTP)Fe^{III}(C≡CPh)} is shown in the Curie plot presented in Figure 8. On warming the sample shows changes that follow the Curie law. Even at room temperature the spectrum remains that of low-spin iron(III) complex. Thus pyridine is more strongly bound to {(TTP)Fe^{III}(C≡CPh)} than is THF.

Solutions of {(TTP)Fe^{III}(C≡CR)} and {py(TTP)Fe^{III}(C≡CR)} are not affected by exposure to dioxygen at room temperature. Thus although these acetylide complexes are sensitive to chromatographic conditions, they are stable to oxidation. Comparison with alkyl and aryl iron(III) complexes under similar conditions indicates the following order of reactivity toward dioxygen; {(TTP)Fe^{III}(alkyl)} > {(TTP)Fe^{III}Ph} > {(TTP)Fe^{III}(C≡CR)}. Treatment of {(TTP)Fe^{III}(C≡CPh)} with bromine at 25° or at −80 °C in toluene-d_8 solution results in the formation of {(TTP)Fe^{III}Br}. No evidence for the formation of a Fe(IV) complex that would correspond to {Br(TPP)Fe^{IV}Ph} which is formed by bromine oxidation of {(TPP)Fe^{III}Ph}[8] has been found.

Discussion

These results establish the existence of two classes of five-coordinate porphyrin complexes with axial acetylide ligands: diamagnetic {PGa^{III}(C≡CPh)} and paramagnetic {PFe^{III}-(C≡CR)}. The fully structurally characterized gallium complexes serve as models for the less robust iron(III) complexes which have proven difficult to purify. Despite their sensitivity during chromatography, these iron acetylide complexes are remarkably stable to oxidation when compared to other iron complexes with Fe–C axial bonds.

The ^{1}H NMR spectral data for {(TTP)Fe^{III}(C≡CPh)} and {(TTP)Fe^{III}(C≡CPr^n)} in noncoordinating solvents indicate that these are high-spin species. The NMR spectral pattern closely corresponds to that of {(TTP)Fe^{III}(OPh)}[9] as can be seen by referring to Table II. In particular the pattern of resonances for the axial aryl protons are similar with the *ortho*- and *para*-phenyl resonances shifted upfield and *meta* resonances shifted downfield. This pattern of shifts reflects the presence of π unpaired spin density on the aryl groups in both cases.

The ^{1}H NMR spectra of the iron(III) acetylide complexes are markedly affected by the presence of coordinating solvent (THF or py). For both solvents, coordination to give six-coordinate species as shown in eqs 1 and 2 is occurring. As expected, the

$$\underset{S = {}^5/_2}{\{PFe^{III}(C{\equiv}CR)\}} + THF \rightleftharpoons \underset{S = {}^1/_2}{\{(THF)PFe^{III}(C{\equiv}CR)\}} \quad (1)$$

$$\underset{S = {}^5/_2}{\{PFe^{III}(C{\equiv}CR)\}} + py \rightleftharpoons \underset{S = {}^1/_2}{\{(py)PFe^{III}(C{\equiv}CR)\}} \quad (2)$$

equilibrium binding of pyridine is stronger, and so at room temperature, it is easily possible to add sufficient pyridine to convert the sample into the six-coordinate form. For THF addition at room temperature both the five- and six-coordinate forms are in rapid equilibrium so that the ^{1}H NMR spectrum (Figure 4, Trace B) appears as the average of the two species present. With THF, cooling does favor formation of the six-coordinate species. The ^{1}H NMR spectral patterns for these six-coordinate adducts are indicative of the presence of low-spin ($S = {}^1/_2$) species. They resemble those of {PFe^{III}Ph} and {(Im)PFe^{III}Ph}.[8,18] The resonances of the aryl groups are indicative of the presence of π unpaired spin density on these axial ligands.

In comparison with the alkyl and aryl complexes, these acetylide complexes of gallium(III) and iron(III) appear to have characteristics of a more ionic M–C bond. This is seen both in the electronic spectra of the gallium complexes, which resemble complexes with axial halide or hydroxide rather than alkyl ligands, and in the high-spin nature of the iron complexes.

Experimental Section

Materials. Toluene, *n*-hexane (dried over potassium and sodium respectively), toluene-d_8, dichloromethane-d_2, and pyridine-d_5 were deoxygenated by three freeze–pump–thaw cycles and stored over 4-Å sieves in a Vacuum Atmospheres glovebox under purified nitrogen. Lithium phenylacetylide in tetrahydrofuran was purchased from Aldrich Chemical Co.

Lithium Propylacetylide. A solution of 5.0 mL of 1-pentyne (Aldrich, 99% purity) in 15 mL of dry *n*-hexane was degassed by bubbling nitrogen through it for 15 minutes. After degassing, the solution was maintained under an atmosphere of dry nitrogen. The solution was then chilled in an ice bath and 31.3 mL of 1.6 M *n*-butyllithium in *n*-hexane (Sure-seal, Aldrich) was slowly added by syringe over the course of one minute. The lithium propylacetylide immediately precipitated as a pale, yellow solid. The reaction was allowed to proceed for 15 minutes before removing it,

Table V. Crystal Structure Data for {(TPP)Ga^{III}(C≡CPr^n)}

$C_{49}H_{35}GaN_4$	fw = 749.5
a = 12.032(2) Å	$Pna2_1$, orthorhombic
b = 27.502(5) Å	T = 120 K
c = 11.138(2) Å	λ(Mo Kα) = 0.710 73 Å
V = 3687(1) Å^3	μ = 0.788 mm^{-1}
Z = 4	d_{calc} = 1.350 Mg/M^3
$R(F)^a$ = 0.043	transm factors = 0.97–0.98
$R_w(F)^b$ = 0.040	

$^a R = \Sigma\|F_o| - |F_c\|/\Sigma|F_o|$. $^b R_w = \Sigma\|F_o| - |F_c\|\sqrt{w}/\Sigma|F_o|\sqrt{w}$.

still sealed, from the nitrogen line and immediately taking in into an inert atmosphere glovebox. Inside the glovebox, the solid product was collected by filtration and washed with dry, degassed *n*-hexane. The solid was then allowed to dry inside the glovebox for 30 minutes, and stored as a solid for later use.

{(TPP)Ga^{III}(C≡CR)} (R = *n*-Pr, Ph). A five-fold molar excess of the appropriate lithium acetylide in dry THF (140 μL of a 1.0 M solution) was added to a solution of 20 mg of {(TPP)Ga^{III}Cl} in 15 mL of toluene under a dinitrogen atmosphere. The pink solution immediately turned violet. The sample was stirred for 5 min, and then the solvent was removed under vacuum. Purification was achieved by dissolving the solid in a minimum amount of benzene and then subjecting this solution to chromatography on a 15 × 2.5 cm grade I basic alumina column. Elution with benzene produced a yellow/violet band which was collected and vacuum dried to give a 33% yield of product. ({(TPP)Ga^{III}Cl} remained on the column as a pink band. It could be removed by treatment with a 1% solution of methanol in chloroform.) The dried product was recrystallized from benzene/*n*-hexane (for R = Pr) or *n*-hexane/diethyl ether (R = Ph) to give a 33% yield of product.

{(TTP)Fe^{III}(C≡CR)} (R = *n*-Pr, Ph). Samples of {(TTP)Fe^{III}(C≡CR)} were best prepared in situ in 5 mm tubes for observation by ^{1}H NMR spectroscopy. Samples of {(TTP)Fe^{III}Cl} (8 mg) were placed in 5 mm NMR tubes and taken into a glovebox under a dry nitrogen atmosphere. Approximately 1 mL of dry, deuterated solvent was added to the NMR tube, and then the tube was sealed with a rubber septum and covered with parafilm. The acetylide complexes formed quickly upon addition of the lithium acetylide in THF to the NMR tube and the red color of the sample became brighter and more vibrant. The lithium reagent was added stepwise in 2 μL aliquots and the progress of the reaction was monitored by ^{1}H NMR spectroscopy. The reactions showed mainly the conversion of {(TTP)Fe^{III}Cl} to {(TTP)Fe^{III}(C≡CR)} but some {(TTP)Fe^{II})} also appeared before all of the {(TTP)Fe^{III}Cl} reacted. {((TTP)Fe^{III})$_2$O} was also present as an impurity. The {(TTP)Fe^{III}C$_2$R} compounds could not be purified by chromatography under a N_2 atmosphere on grade I basic or neutral alumina, or silica gel owing to degradation on the column to form {(TTP)Fe^{II}}. Recrystallization afforded no further purification from trace porphyrin impurities. These compounds did not react readily with dioxygen, but did degrade slowly in the presence of water. The purest product was obtained by in situ NMR titration followed by decanting the solution out of the NMR tube into an oven dried Schlenk tube so that any residual solid material was left behind in the NMR tube. The sample was then vacuum dried. This procedure allowed for the removal of the THF and insoluble side products while maintaining the integrity of the desired product. The sample could then be redissolved and studied in a variety of solvent systems.

X-ray Data Collection for {(TPP)Ga^{III}(C≡CPr^n)}. Blood red blocks were obtained by diffusion of hexane into a benzene solution of the complex. A suitable crystal was coated with a light hydrocarbon oil and mounted in the 130 K dinitrogen stream of a Siemens R3m/v diffractometer equipped with a Enraf-Nonius low temperature apparatus. Two check reflections showed random (<2%) variation during data collection. The data were corrected for Lorentz and polarization effects. Crystal data are given in Table V.

Solution and Refinement of the Structure. Calculations were performed on a DEC VAX station 3200 with the programs of SHELXTL Plus v. 4.0. Scattering factors for neutral atoms and corrections for anomalous dispersion were taken from a standard source.[34] The solution of the structure was obtained by Patterson synthesis. During the last stages of refinement all the non-hydrogen atoms were assigned anisotropic thermal parameters. Hydrogen atoms were located on a difference map and fixed at ideal geometries for subsequent cycles of least squares refinement.

Instrumentation. ^{1}H NMR spectra were recorded at 300 MHz on a General Electric QE-300 Fourier transform spectrometer. Spectra of paramagnetic complexes were collected over a 30–70-kHz bandwidth with 16 K data points. Between 500 and 10 000 transients were accumulated with a delay time of 50 ms. Spectra of diamagnetic samples were collected over a 6–10-kHz bandwidth with 32 K data points. Between 100 and 300 transients were accumulated with a delay time of 1 sec. Electronic absorption spectra were obtained through the use of a Hewlett-Packard 9122 diode array spectrometer.

Acknowledgment. We thank the NIH (Grant GM26226) for financial support.

Supplementary Material Available: Tables of crystal data, bond distances, bond angles, anisotropic thermal parameters, and hydrogen atom coordinates for {(TPP)Ga^{III}(C≡CPr^n)} (9 pages). Ordering information is given on any current masthead page.

(34) *International Tables for X-ray Crystallography*; Kynoch Press: Birmingham, England, 1974; Vol. 4.